LARVICIDAL, ANTIMICROBIAL AND EXTRACTIVE PROPERTIES OF AMINO-BASED SCHIFF BASES AND THEIR COMPLEXES: SYNTHESIS, CHARACTERIZATIONS, DFT AND MOLECULAR DOCKING STUDIES

FESTUS CHIOMA[1*] AND CHIOMA D. DON-LAWSON[2]

[1]Department of Chemistry, Faculty of Natural and Applied Sciences, Ignatius Ajuru University of Education Rivers State, Nigeria.

[2]Department of Science Laboratory Technology, School of Science and Technology, Port Harcourt Polytechnic, Nigeria.

AUTHORS' CONTRIBUTIONS

This work was carried out in collaboration between both authors. Author FC designed the research, synthesized the chelator plus chelates with the help of author CDDL. Author FC characterized and analyzed all compounds, and wrote the manuscript. Author CDDL proofread the manuscript. Both authors read and approved the final manuscript.

ABSTRACT

Aims: This study is targeted at the synthesis of a new imine-chelator and its Fe^{2+}, Ni^{2+} and Cu^{2+} chelates derived from 2-hydroxyl-1-naphthaldehyde and 2-amino-4-methylphenol for characterization and; for bactericidal, anti-fungiform, antioxidant and extractive potentials' evaluations.Spectral (UV/visible, vibrational, plus nuclear magnetic resonance) methods, analytical (C, H, N, Melting point, magnetic susceptibility, and conductance, complexometric) techniques and biological (antimicrobial, antioxidant plus extractive potentials) appraisals were all adopted for the study of the synthesized chelator and its chelates. A new-fangled heterocyclic chelator, 3-[(2-hydroxy-5-methylphenylimino)-methyl]-napthalen-2-ol and its Fe^{2+}, Ni^{2+} and Cu^{2+} chelates were synthesized and characterized with proton nuclear magnetic resonance (^{1}H NMR), vibrational (FT-IR), mass (ESI-MS) and electronic spectral techniques; in addition to micro (C,H,N)analysis, magnetic susceptibility (μ_{eff}), plus molar conductance evaluations. The acquired FT-IR spectral values denoted excellent chelation attributes of the chelator towards the 3d-M^{2+} ions through the deprotonated oxygenand imine nitrogen atoms. The structural assemblages leading to the geometries (octahedral, square planar plus tetrahedral for Fe^{2+}, Cu^{2+} and Ni^{2+} chelates) were deduced from experimental data arising from C,H,N-analysis, μ_{eff} , plus electronic spectral evaluations. In addition to the latter, the ^{1}H NMR plus ESI-MS values provided the basis for the proposed structure of the chelator. Molar conductance data validated the neutrality of the chelates. The acquired ESI-MS spectrum presented convincing fragmentation pathways, stoichiometric contents, as well as formula weight for the chelator. The in vitro antimicrobial actions of the compounds against isolated microbial strains exhibited altered actions. The $[Fe(C_{36}H_{32}N_2O_6)]$ demonstrated superlative antimicrobial actions against all the tested microbes with inhibitory growth zones comparable to that of the adopted standard drugs. The compounds presented excellent DPPH antioxidant scavenging actions, with the $[Ni(C_{36}H_{30}N_2O_5)]$ chelate having the most outstanding antioxidant action with an IC_{50} of 98%, IC_{100} of 99% and IC_{200} of 99% compared to others.

Keywords: Imine-chelator; antioxidant; nuclear magnetic resonance and fragmentation pathways.

1. INTRODUCTION

Chelators consisting of imine moiety in addition to O, N, S atoms within their structural assemblages have gained prominence amid researchers in the field of coordination chemistry [1] owing to their pharmacological actions. The heteroatoms (N, O, S) are acknowledged as the propelling force for the exceptional binding potentials of imine bearing chelators often exhibited towards metallic ions [2,3] in chelate formation [4]. The latter have been reported to possess distinct physiological, morphological, and pharmacological actions compared to their chelators, a consequence of the integrated metallic species within the

framework of the former [2,5]. Heterocyclic based chelators recently have attracted favorable research awareness due to their likely usage as agents for antimicrobial resistance, metallic ions' extraction, electrochemical plus quantum chemical assessments of steel erosion, etc [6,7,8]. Documented reports shows that Heterocyclic imine-based chelates exhibit better valuable pharmacological actions [9,10,2] in addition to their strong catalytic, extractive and surfactant activities in countless chemical reactions [11,12] than their precursors. Also, with countless research reports on the inclusion of metallic species in medications, several biological molecules consisting of hydroxyl moiety as a fragment of their structural assemblage exhibit enzyme-based actions in addition to their varied biological concerns. This current study, is dedicated to the synthesis plus characterization of a new imine-chelator and its Fe^{2+}, Ni^{2+} and Cu^{2+} chelates derived from 2-hydroxyl-1-naphthaldehyde and 2-amino-4-methylphenol. The spectral, bactericidal, anti-fungiform, antioxidant actions of the compounds, in addition to the extractive potentials of the chelator were examined.

2. EXPERIMENTAL SECTION

2.1 Materials and Methods

All chemicals/solvents were purchased and used at reagent standard from BDHs plus Sigma-Aldrich without purifications. The Bruker Avance III 300 MHz, Lambda 25 UV/visible plus Perkin-Elmer spectrum-2000 FTIR spectrophotometers were utilized for FT-IR, electronic plus NMR spectral appraisals. While the NMR spectra stood acquired in deuterated d6-$(CH_3)_2SO$ solvent with tetramethylsilane (TMS) as internal standard, the FT-IR spectra were obtained as KBr pellets and the electronic spectra remained acquired as solid reflectance. The synthesized chelator plus its chelates were examined for elemental C, H, N compositions on Perkin Elmer CHNS/O 2400 version II elemental analyser. A see-through cut-glass hose fitted into an Electro-thermal M-Pt device was adopted to acquire the melting points values for the synthesized compounds. The magnetic susceptibility (μ_{eff}) and conductance evaluations were acquired according to a reported procedure [13]. Similarly, the percentage metal ion contents in the chelates were acquired complexometrically in EDTA. The ESI-MS of the chelator stood acquired via dissolution of a little amount of the sample in few droplets of CH_2Cl_2, accompanied with dilution to ± 2 mL by CH_3OH. The ESI-MS data obtained in a positive ion mode via pneumatically aided electro-spray ionization: 2900 V-capillary voltage; 15 V- sample cone voltage;, 1 V-extraction voltage; 80°C- source temperature; 160°C-desolvation temperature; 100 L h^{-1}- cone gas flow; 100 L h^{-1}- desolvation gas flow; 2 V- collision voltage; 2400 V- MCP voltage.

2.2 Synthesis of Imine Chelator

The imine chelator was synthesized following an earlier reported procedure for comparable chelators [14,15]. The starting materials were first mixed together and then refluxed with an acetic acid to afford the wanted imine chelator as shown in scheme 1.

2.3 Synthesis of M(II) Chelates

An ethanolic mixture (25 mL) of the suitable M(II) acetate salts $Cu(CH_3COO)_2.H_2O$ (0.11 g) plus $Ni(CH_3COO)_2.4H_2O$ (0.12 g); and sulphate salt $FeSO_4.7H_2O$ (0.15 g) separately were reacted with an equivalent mole of the imine chelator (0. 3 g). Reflux of the mixture with $(C_2H_5)_3N$ lasted for 4 h at 55 ^{0}C. The resultant precipitates were individually collected by gravity filtration, recrystallized from warm ethanol and desiccated over $CaCl_2$ for 48 h before further analyses.

2.4 Antimicrobial Evaluations

The antimicrobial activities of the synthesized imine chelator plus its M(II) chelates stood appraised for anti-bacteriological in addition to anti-fungiform possibilities through well diffusion method. The stains; E. coli, S. aureus, B. cereus plus P. aeruginosa; A. niger as well as F. specie were incubated for 24 h and 48 h separately at 37◦C and used. The drugs ciprofloxacin with fluconazole were adopted as non-negative standards. All other procedures were directly followed as reported in our previous publications [16] with simple mean and

standard deviation adopted for the analysis of the acquired data.

2.5 Antioxidant Studies

The chelator and its chelates were appraised for free radical scavenging action with using 2,2-diphenyl-1-picryl-hydrazyl ($C_{18}H_{12}N_5O_6$) practice. Altered concentrations; 200, 100 plus 50 "g/mL with 0.4 mL of the synthesised chelator and its chelates were made in 2.6 mL of 0.025 g/L $C_{18}H_{12}N_5O_6$ in dimethyl-sulphoxide ($(CH_3)_2SO$). All solutions prepared were vigorously mixed, and equilibrated for 45 min at laboratory temperature. The procedure reported by [8] was adopted for the preparation of the control as well as the determination of the absorbance of the solutions. The reduction of $C_{18}H_{12}N_5O_6$ stood estimated in relation to acquired absorbance for the control.

3. RESULTS AND DISCUSSION

3.1 Chemistry

Three new homoleptic chelates ofFe^{2+}, Ni^{2+} plus Cu^{2+} species with an N,O hydroxyl-phenol chelator, 3-[(2-hydroxy-5-methylphenylimino)-methyl]-napthalen-2-ol were synthesized through reflux-condensation technique in alcoholic solvent. The chelates as well as the chelator were acquired in a 1:1 mole-ratio from the precursor reagents and in moderate to excellent yields. All proposed structural assemblages (chelator plus chelates) were on the basis of investigational, spectroscopic in addition to magnetic susceptibility data. The chelator plus its chelates were intensely colored with firmness at all temperatures.

3.2 ESI-MS Studies

Fig. 1 is the acquired ESI-M spectrum for the synthesized chelator with the condensed formula of $C_{18}H_{15}NO_2$. The fragmentation outline plus stoichiometric fragments of the chelator has been proposed from the spectrum and presented as scheme 2. The latter conforms to rudimentary contents of C, H, N obtained through micro-analysis. The peak noticed for molecular ion (m^+.) around m/z 273 arose from an $(L)^+$ loss of 3H atoms conforming to the formula weight of 277.316 g/mol of the chelator. In general the chelator displayed twofold disintegration paths giving rise to diverse fragments which in turn substantiates the reflux condensation of 2-hydroxyl-1-naphthaldehyde and 2-amino-4-methylphenol to afford the chelator. In addition to the observed molecular ion signal, the chelator had other peaks corresponding to the ions; $[C_2H; m/z = 25.028]^+$, [HO; $m/z = 17.006]^+$, $[C_2H_2O; m/z = 42.034]^+$, $[C_4N; m/z = 62.05]^+$; plus $[CH_4O; m/z = 32.04]^+$, $[C_6HN; 87.078]$, as well as $[CHO; m/z = 29.016]^+$ at m/z 249.264, 232.258, 190.224, 128.174; 242.033, 155.079 plus 126.158 separately.

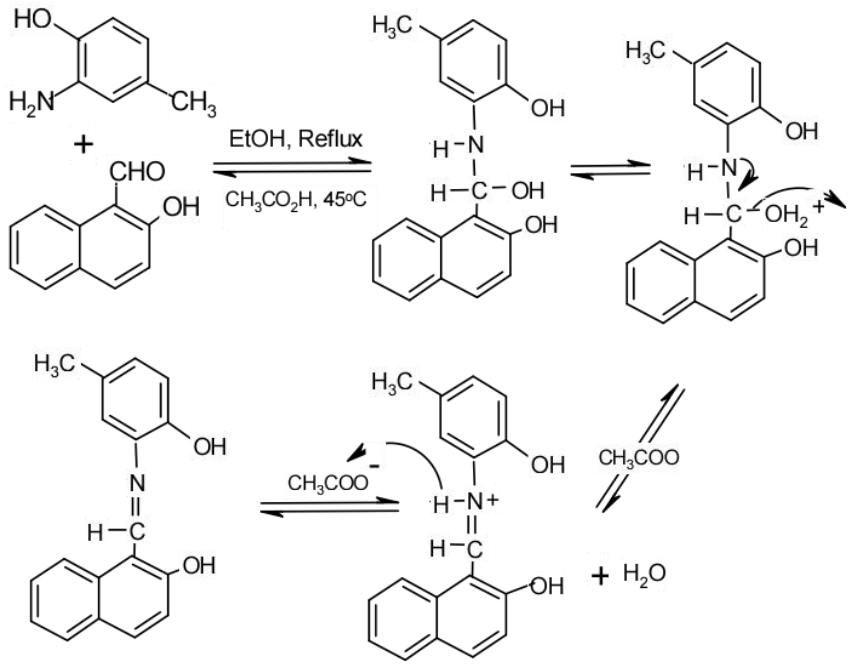

Scheme 1. Steps for the synthesis/proposed assemblage of the chelator

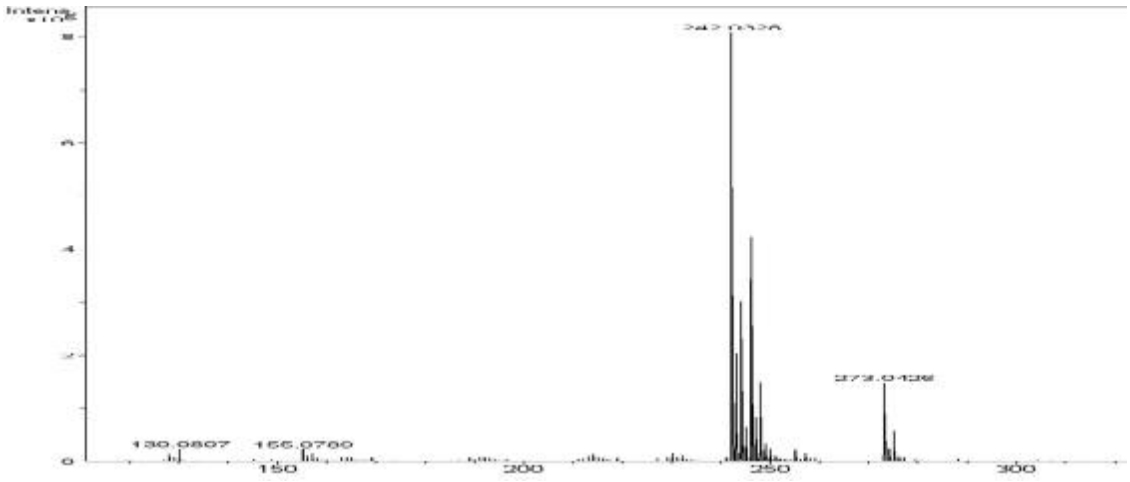

Fig. 1. Electrospray ionization spectrum of the chelator

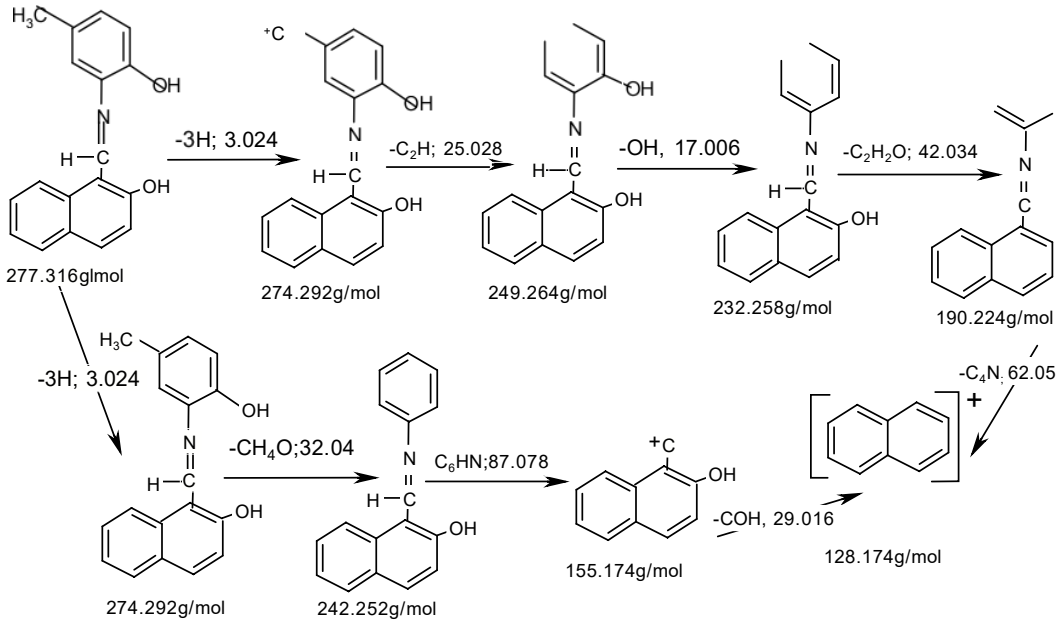

Scheme 2. Fragmentation pathways of the chelator

3.3 Magnetic Susceptibility (μ_{eff}) and Molar Conductivity Measurements

All synthesized chelates were assessed for μ_{eff} amid 298–305 K. The effective μ_{eff} of a high spin magnetically dilute divalent iron chelates are predictable to have values ranged from 5.0 B.M to 5.5 B.M regardless of stereochemistry owing to orbital contributions and spin-orbit coupling effects with exceptions only detected in spin crossover environments [17,18], presence of associated antiferromagnetic interaction [19]. So, obtained 5.41 B.M magnetic data for our divalent iron chelate ruled-out metal-metal interaction within the chelate complex but was complimentary of distorted octahedral geometry [20]. Though, we didn't explore further owing to inadequate facilities for variable-temperature μ_{eff} evaluations. The μ_{eff} data for Ni^{2+} chelates ordinarily remain less than or approximately one for square planar geometry, a consequence of their magnetically dilute nature [21,3]. Nonetheless, non-magnetically dilute tetrahedral Ni^{2+} chelates displays μ_{eff} figures of 3.20-4.20 B.M [22,23]. A μ_{eff} value of 4.53 B.M was obtained for the synthesized Ni^{2+} chelate authenticating non-low spin tetrahedral structure assigned to it knowing that octahedral Ni^{2+}

chelates are projected to exhibit 2.90 – 3.30 BM μ_{eff} values. Investigational reports often reveal μ_{eff} data of 1.9-2.2 BM for non-binuclear Cu^{2+} chelates, regardless of stereochemistry, predictably larger compared to spin single μ_{eff} of 1.73 BM arising from orbital contribution plus spin-orbit coupling effects [24]. The 2.14 B.M μ_{eff} data denotes non-magnetically dilute plus non-binuclear nature of the synthesized Cu^{2+} chelate. The molar conductivity ($ohm^{-1}mol^{-1}cm^2$) capacities evaluated in ($(CH_3)_2SO$) solvent designated data for the synthesized Fe^{2+} as 31.1 $ohm^{-1}cm^2mol^{-1}$, Ni^{2+} as 21.6 $ohm^{-1}cm^2mol^{-1}$ plus Cu^{2+} as 7.92 $ohm^{-1}cm^2mol^{-1}$ chelates singly. Therefore, the ohm-1mol-1cm2 data corroborates the chelates as non-electrolytes [25], as values beyond 40 $ohm^{-1}cm^2mol^{-1}$ and 90 $ohm^{-1}cm^2mol^{-1}$ stood commonly appraised for 1:1 and 2:1 electrolytes correspondingly [3,26] and are presented in Table 1.

3.4 NMR Studies

The acquired proton-NMR spectrum (Fig. 2) of the chelator displayed a medium-sized singlet peak at 2.49 ppm was apportioned to methyl (CH_3) protons on the hydroxyl phenol ring. The hydrogen atoms of the cyclic methyl-phenol moiety appeared as a strong peak at 6.15ppm with other small-sized peaks at 7.76ppm, 7.77ppm, and 7.78 ppm, whereas the aromatic protons of the fused naphthalene ring resonated as doublets at 7.98ppm, 7.96ppm, 7.92ppm and 7.80ppm. Additionally, the proton peak arising from the imine function was seen as a singlet at 8.25ppm, a corroborative evidence for the formation of the chelator. The resonance signals at 9.17 ppm plus 8.84-8.64 ppm stood assigned to the presence of OH protons of the hydroxyl moieties separately.

Table 1. Analytical figures for the chelator and its chelates

Chelator/ Chelates	Colour	Molecular Mass	$ohm^{-1}cm^2mol^{-1}$	μ_{eff} (BM)	Melting point	Micro-Analysis (observed/theo)			
						C	H	N	M
HL, $[C_{18}H_{15}NO_2]$	Orange	277.316	_		324	77.91/ 77.95	5.39/ 5.45	5.09/ 5.05	_
$[Fe(C_{36}H_{32}N_2O_6)]$	Black	644.484	31.1	5.41	389	67.03/ 67.08	4.31/ 4.35	4.31/ 4.35	8.64/ 8.67
$[Ni(C_{36}H_{30}N_2O_5)]$	Orange	629.32	21.6	4.53	279	68.66/ 68.69	4.79/ 4.80	4.41/ 4.44	9.38/ 9.35
$[Cu(C_{32}H_{28}N_2O_4)]$	Greenish orange	616.136	7.92	2.14	290	70.14/ 70.17	4.56/ 4.58	4.52/ 4.55	10.28/ 10.31

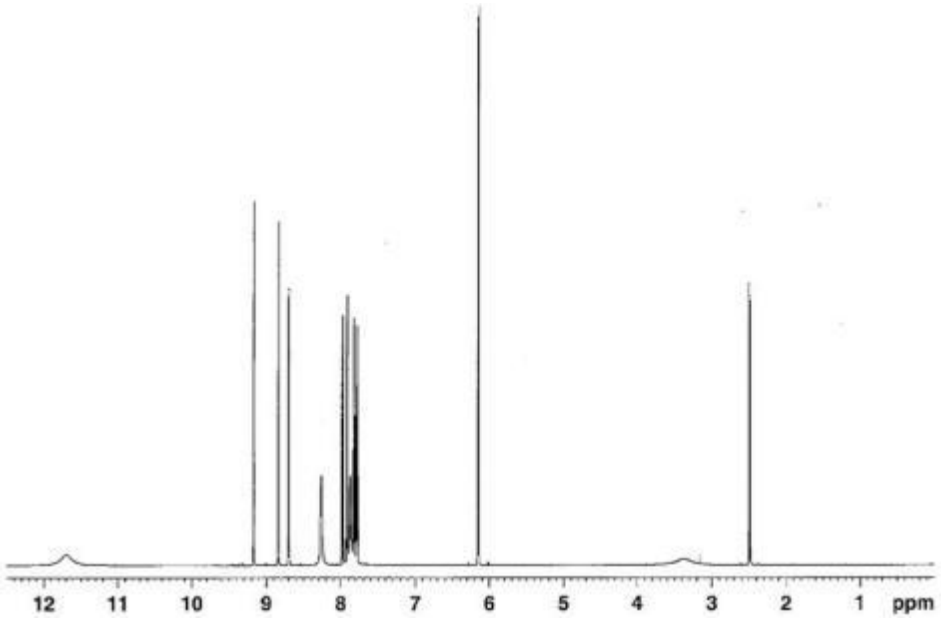

Fig. 2. ^{1}HNMR spectrum of the chelator

3.5 Electronic Spectral Studies

Acquired electronic spectral statistics for the compounds are contained in Table 2. The electronic signals amid 27933–28490cm^{-1} plus 31153–39063cm^{-1} in the chelator's spectrum were corroborative of the transitions; $n \rightarrow \pi^*$ in addition to $\pi \rightarrow \pi^*$. Whereas the latter resulted from the ring effects of the imine chelator-aromatic carbon carbon double bonds, the non-bonded electrons resident on the nitrogen atom of the imine moiety gave rise to the former corroborating electron transfer ($n \rightarrow \pi^*$) from non-bonded pairs of electron to an anti-bonding (σ^*) orbital [27,11]. Bivalent iron chelates frequently exhibit only one spin allowed transition, $t_{2g}^4 e_g^2 ({}^5T_{2g}) \rightarrow t_{2g}^3 e_g^3 ({}^5E_g)$ but are often subjects to further splitting arising from Jahn Teller distortions with ${}^5T_{2g} \rightarrow {}^5A_{1g}$ and ${}^5T_{2g} \rightarrow {}^5B_{1g}$ transitions in the octahedral field [28]. The Fe^{2+} chelate under study had signals around 19230 cm^{-1} as well as 18248-18903 cm^{-1} typical of ${}^5T_{2g} \rightarrow {}^5A_{1g}$ plus ${}^5T_{2g} \rightarrow {}^5B_{1g}$ transitions, suggestive of a distorted octahedral geometry. Three absorption bands apportioned to $n \rightarrow \pi^*$, $\pi \rightarrow \pi^*$ in addition to charge transfer transitions (CTTs) were observed at 27855 cm^{-1} plus 33783-39525 cm^{-1}. The Ni^{2+} chelate under study presented signals conforming to a tetrahedral assemblage at 13123 cm^{-1} plus 23923 cm^{-1} allotted to ${}^3T_1(F) \rightarrow {}^3T_2$, as well as ${}^3T_1(F) \rightarrow {}^3A_2$ transitions [29] as expected of non-low spin Ni^{2+} chelates amid visible electronic regions. Enhanced energy signals detected from 32679–33783 cm^{-1} remained consistent of M→L CTTs. Assigned assemblage was further substantiated by the chelator field parameters. For example, the B_1 values for the synthesized Ni^{2+} chelate were lesser compared to the free ion figures, indicative of orbital intersection in addition to re-arrangement of d- orbital electrons. Also obtained values for the β parameter were somewhat lesser compared to normal, signifying a substantial amount of hybridization amid the bonds operative between the chelate ion with its chelator. The Ni^{2+} chelate in its non-visible spectrum presented twofold signals allocated to $\pi^* \leftarrow n$ (25518 cm^{-1}) as well as $\pi^* \leftarrow \pi$ (33783 cm^{-1}) transitions. The synthesized Cu^{2+} chelate displayed band at 20212 cm^{-1} suggestive of distorted four-coordinate square-planar geometry of ${}^2B_{1g} \rightarrow {}^2A_{1g}$ and ${}^2B_{1g} \rightarrow {}^2E_{1g}$ transitions [30,31], knowing that tetrahedral divalent copper chelates typically exhibits a single absorption band below 10000 cm^{-1} while a lone band above 10000 cm^{-1} within the octahedral environment is often observed. Two electronic bands detected at 29002 cm^{-1} and 30675 - 33898 cm^{-1} in the UV spectrum indicate $\pi \rightarrow \pi^*$ and $n \rightarrow \pi^*$ transitions.

3.6 Vibrational (FT-IR) Studies

Table 3 contains all pertinent vibrational bands acquired for the chelator and chelates apportioned on association with related system(s) cited in literature. A noticeable band within the spectrum of the chelator at 3336cm^{-1} was apportioned to vibrational stretch consistent with an -OH functional group. The latter remained non-existent in the spectra of the chelates confirmative of displacement of –H atom with consequent bonding of the resulting electronegative enol -O atom in chelation. The wavenumbers arising from unbounded carbon nitrogen plus carbon carbon double bonds vibrational stretches resonated as combined bands amid 1633- 1602cm^{-1} in the chelator [32,33] but suffered somewhat shifts to 1615-1598 cm^{-1} on chelation with each M^{2+} specie. The carbon carbon double denotes presence of the imine-N in chelation [34,13]. The vibrational bands related to aromatic carbon hydrogen single bond stretches were spotted amid 3059 cm^{-1} to 2994 cm^{-1} in the chelator

Table 2. Electronic spectra

Chelator/Chelates	Absorption Bands(cm^{-1})	Transition(s)/Band Assignment	Geometry
HL, $[C_{18}H_{15}NO_2]$	27933, 28490 31153, 39063	n - π * π - π *	-
$[Fe(C_{36}H_{32}N_2O_6)]$	19230, 18248, 18903, 27855, 33783	${}^5T_{2g} \rightarrow {}^5A_{1g}$, ${}^5T_{2g} \rightarrow {}^5B_{1g}$ n - π * π - π *	Octahedral
$[Ni(C_{36}H_{30}N_2O_5)]$	13123, 23923, 25518, 33783	${}^3T_1(F) \rightarrow {}^3T_2$, ${}^3T_1(F) \rightarrow {}^3A_2$ n - π * π - π *	Tetrahedral
$[Cu(C_{32}H_{28}N_2O_4)]$	20212, 29002, 30675, 33898	${}^2B_{1g} \rightarrow {}^2A_{1g}$, ${}^2B_{1g} \rightarrow {}^2E_{1g}$ n - π * π - π *	Square planner

Table 3. Vibrational Spectral Data for the prepared compound (cm^{-1})

Compound	OH	C=N	C-N	C=C	C-C	C-O	C-H	CH_3	M-O	M-N
HL, $[C_{18}H_{15}NO_2]$	3336	1633	1546	1602	1224	1352	3114	2914	-	-
$[Cu(C_{32}H_{28}N_2O_4)]$	2428	1615	1535	1599	1230	1339	3058	2914	464	503
$[Fe(C_{36}H_{32}N_2O_6)]$	3405	1615	1532	1598	1226	1341	3055	2919	471	551
$[Ni(C_{36}H_{30}N_2O_5)]$	3260	1614	1532	1601	1230	1356	3054	2915	459	507

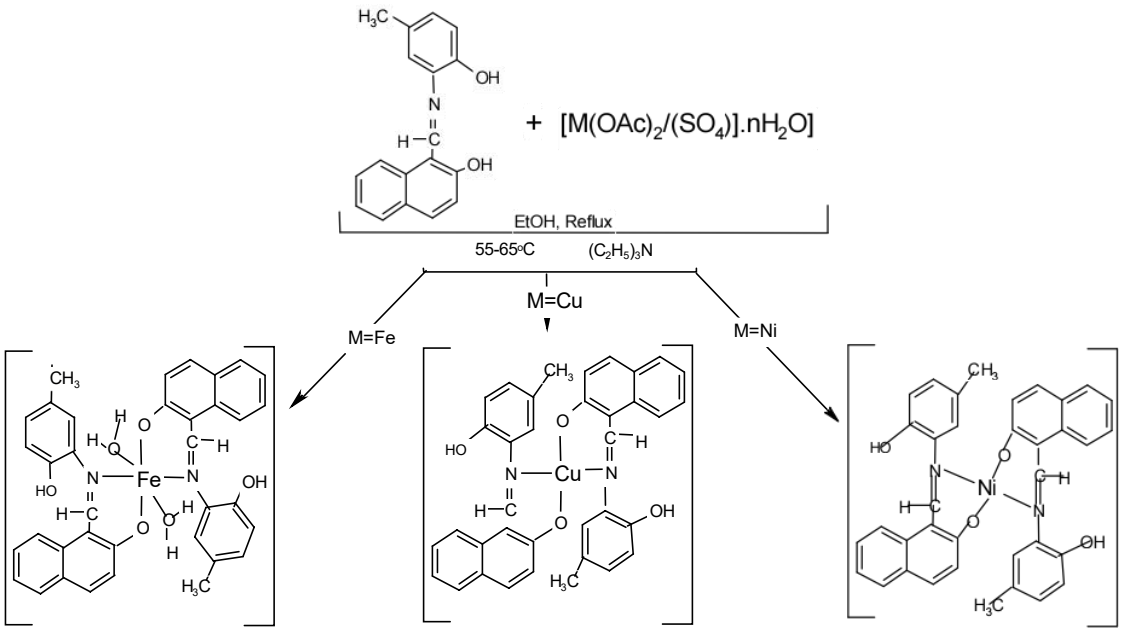

Scheme 3. Synthetic procedure for the chelates and their proposed structures

[11] as well as the chelates; whereas the non-cyclic carbon hydrogen single bond vibrations consistent of CH_3 moiety resonated from 2919-2914cm^{-1}. The vibrational stretches noticed from 1387-1352cm^{-1} were credited to carbon oxygen single bond vibrations within the chelator spectrum, nonetheless minor shifts within the spectra of the chelates, a consequence of chelation influence [30,14]. The chelator spectrum presented signals at 1224 cm^{-1} as well as 1546cm^{-1} conforming vibrations of carbon carbon plus carbon nitrogen single bond stretches distinctly. The carbon nitrogen single bond signal as observed meaningfully shifted to a somewhat wavenumbers, symbolic of chelation impact but the carbon carbon single bond signal maintained its stretching positions in the spectrum of the chelates. Noticeable non-chelator bands amid 459-471 cm^{-1} in addition to 503-551 cm^{-1} were apportioned to vibrations of metal oxygen plus metal nitrogen stretches within the spectra of the chelates [32] substantiating the enol oxygen atom plus imine nitrogen atom participation in chelation with M^{2+} species. This corroborates movement of electron(s) resident on N- of the imine group to an unoccupied M^{2+} d-orbitals giving rise to M-N bond establishment, thereby causing C=N band weakening as noticed in carbon nitrogen double bond stretching values [35,27].

3.7 Applied Studies

3.7.1 Antimicrobial appraisals

The chelator had no antimicrobial actions against S. aureus, P. aeruginosa, B. cereus, plus A. niger, except against E, coli, and F. specie with inhibitory growth zones of 12.05 and 9.10mm separately. The chelator's inactivity towards the screened species is attributable to prompt creation of persuasive poisons by the microbes triggering activation of the bacteriological-cell superficial proteins thereby inhibiting apt infiltration of the synthesized chelator to designated bacteriological-cells. Effect of the bacteriological persuasive poisons is believed to have reduced the lipophilic potentials of the chelator hence diminishing the chelator's permeation [36,37]. Largely, all synthesized chelates presented different sorts of bacteriological action against all tested species which could be arising from chelation effect known for easing penetrability obstruction into the cell, giving rise to the interference with the usual cellular

workings [38]. The Ni^{2+} chelate remained sensitive against only S. aureus (26.00 mm) and B. cereus (18.00 mm) independently. Equally, the Cu^{2+} chelate had activities values of 24.00mm, 15.50mm, 8.20mm plus 9.00mm against S. aureus P. aeruginosa E, coli plus F., specie separately. The Fe^{2+} chelate substantially showed outstanding activities all screened species in the order S. aureus (31.00 mm), > B. cereus (25.00 mm), > P. aeruginosa (19.00 mm), > E. coli (16.00 mm), > F. specie (9.00 mm) > A. niger (6.00 mm) differently. The implication of the outstanding sensitivity of the synthesized Fe^{2+} chelate denotes the chelate's possibilities in future antimicrobial drug design plus development for the treatment of microbial infections.

3.7.2 Antioxidant assessments

Generally, the adoption and usage of $C_{18}H_{12}N_5O_6$ technique for antioxidant studies of synthesized chelators/chelates as well as natural compounds has remained an efficient-reproducible procedure in countless evaluation involving antioxidant actions [39]. The chelator with its chelates were appraised for antioxidant possibilities using $C_{18}H_{12}N_5O_6$reagent with 200, 100 and 50 g/mL concentrations prepared in 1.0 mL $(CH_3)_2SO$. The acquired data of the $C_{18}H_{12}N_5O_6$ appraisal for the synthesized chelators/chelates are accessible as Fig. 5 and denotes that the compounds are largely excellent $C_{18}H_{12}N_5O_6$ scavenger. The synthesized chelator presented

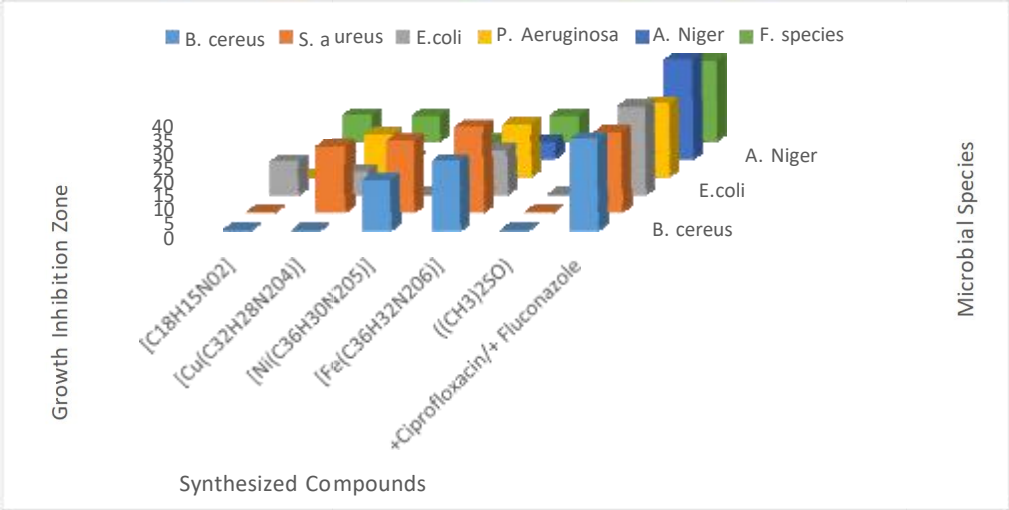

Fig. 4. Histogram of the antimicrobial actions of the chelators and its chelates

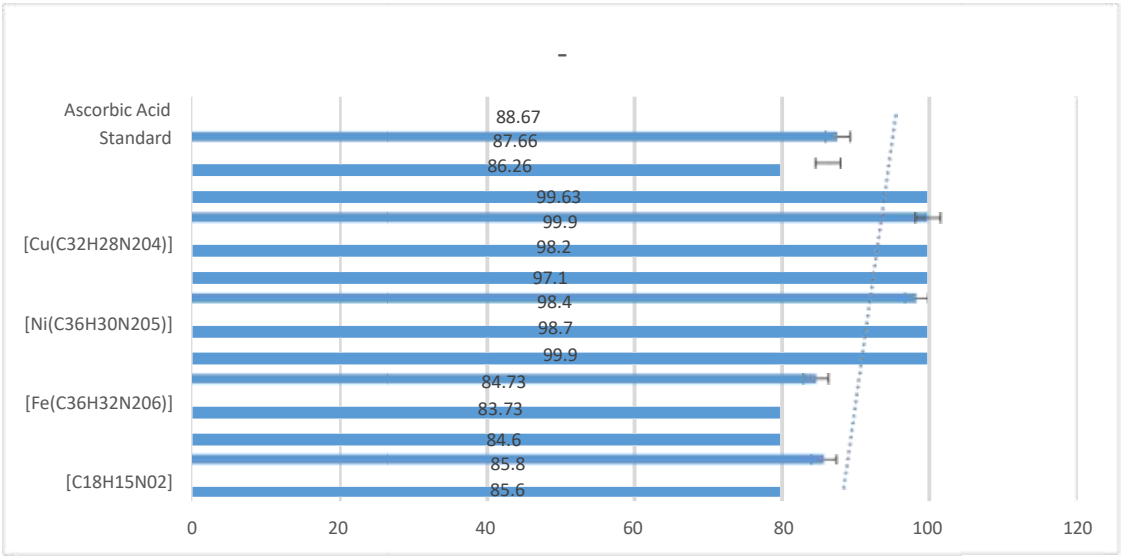

Fig. 5. Graphical representation of the antioxidant actions of the chelator and its chelates

$C_{18}H_{12}N_5O_6$ foraging potential data, however failed lower compared to the ascorbic acid standard used. Conversely, the chelates displayed enhanced antioxidant potentials possibly due to chelation. Usually, chelates are known for improved $C_{18}H_{12}N_5O_6$ foraging actions than their pioneer chelators. Acquired data can be adopted as a guide for frontier research involving design of medications for handling of pathological ailments due to oxidative pressure.

4. CONCLUSION

The chelator; 3-[(2-hydroxy-5-methylphenylimino)-methyl]-napthalen-2-ol was effectively synthesized via reflux-condensation process in an alcoholic medium. Further reaction of the chelator with Fe^{2+}, Ni^{2+} and Cu^{2+} ions afforded the equivalent chelates. Analytical (melting points, μ_{ef}, molar conductance plus micro-analysis), spectral (FT-IR , ^{1}H NMR, ESI-MS plus electronic) and computational (DFT, molecular dockings) methods were adopted for the characterization of the synthesized compounds. The chelator was bi-dentate and exhibited same in chelating with M^{2+} ions. The Fe^{2+}, Cu^{2+} and Ni^{2+} chelates assumed octahedral, square planar plus tetrahedral geometries in addition to their non-ionic natures. The fragmentation pathways, stoichiometric contents, as well as formula weight for the chelator were obtained from the ESI-MS spectrum. The in vitro antimicrobial actions of the compounds against isolated microbial strains exhibited altered actions. The $[Fe(C_{36}H_{32}N_2O_6)]$ demonstrated superlative antimicrobial actions against all the tested microbes with inhibitory growth zones comparable to that of the adopted standard drugs. The compounds presented excellent DPPH antioxidant scavenging actions, with the $[Ni(C_{36}H_{30}N_2O_5)]$ chelate having the most outstanding antioxidant action with an IC_{50} of 98%, IC_{100} of 99% and IC_{200} of 99% compared to others.

ACKNOWLEDGEMENTS

The authors appreciatively thank the Department of Chemistry, Ignatius Ajuru University of Education for giving us all that were required for the experimental works. TETFund (TETFUND/DESS/UNI/RUMUMUMUOLUMENI/2013/VOL. 1) is highly commended for funding of the research.

COMPETING INTERESTS

Authors have declared that no competing interests exist.

REFERENCES

1. Gulcan M, Ozdemir S, D¨undar A, Ispir E, Kurto˘glu M. Mononuclear complexes based on pyrimidine ring azo schiffbase ligand: Synthesis, characterization, antioxidant, antibacterial, and thermal investigations, Zeitschrift fur Anorganische und Allgemeine Chemie. 2014;640(8-9):1754–1762.
Available:https://doi.org/10.1002/zaac.201400078

2. Narendra KC, Parashuram M. Metal Complexes of a Novel Schiff Base Based on Penicillin: Characterization, Molecular Modeling, and Antibacterial Activity Study" Bioinorganic Chemistry and Applications. 2017;1-13.
Available:https://doi.org/10.1155/2017/6927675

3. Festus C, Don-Lawson CD, Ima-Bright N. Synthesis involving asymmetric pyrazine-schiff base with Co^{2+}, Ni^{2+} and Cu^{2+} ions: Spectral and Magnetic Characterization; and Antibacterial studies. Int.l J. of Research & Innovation in Applied Science. 2019;4(4).
Available:www.rsisinternational.org

4. Khlood SAM, Al-Hazmi AG, Althagafi I, Alharbi A, Keshk AA, Shaaban F, El-Metwaly N. Spectral, molecular modeling, and biological activity studies on new schiff's base of Acenaphthaquinone Transition Metal Complexes Bioinorganic Chemistry and Applications. 2021;1-17.
Available:https://doi.org/10.1155/2021

5. Festus C, Ozioma AE, Don-Lawson CD. Novel metal2+ complexes of N-(1,4-dihydro-1,4-oxonaphthalen-3-yl) pyrazine-2-carboxamide: Synthesis, structural characterization, magnetic properties and antimicrobial activities. Curr. Res. Chem. 2020;12:1-10.
DOI: 10.3923/crc.2020.1.10

6. Hasanov R, Sadikoglu M, Bilgic S. Electrochemical and quantum chemical studies of some Schiff bases on the corrosion of steel in H_2SO_4 solution, Appl. Surf. Sci. 2006;253(8):3913e3921.
DOI: 10.1016/j.apsusc.2006.08.025

7. Karem LKA, Waddai FY, Karam NH. Schiff base complexes of some drug substances: Review, J. Pharmaceut. Sci. Res. 2018;10(8):1912-1917.
Karem LKA, Waddai FY, Karam NH. Schiff base complexes of some drug substances: Review, J. Pharmaceut. Sci. Res. 2018;10(8):1912-1917.
Available:https://www.jpsr.pharmainfo.in/Documents/Volumes/vol10Issue08/jpsr

8. Festus C, Don-Lawson CD. Solvothermal synthesis; Analytical and spectral characterization; and solvent extraction studies of heterocyclic schiff base ligands scholarly, Journal of Scientific Research and Essay. 2017;6(6):166-173.
Available:http:// www.scholarly-journals.com/SJSRE

9. Creaven BS, Czeglédi E, Devereux M, Enyedy ÉA, Foltyn-Arfa A, Karcz D, et al. Biological activity and coordination modes of copper(II) complexes of Schiff base-derived coumarin ligands, Dalton Transactions. 2010;39:10854–10865.
DOI: https://doi.org/ 10. 1039/C0DT00068J

10. Manjunatha M, Naik VH, Kulkarni AD, Patil SA. DNA cleavage, antimicrobial, antiinflammatory anthelmintic activities, and spectroscopic studies ofCo(II), Ni(II), and Cu(II) complexes of biologically potential coumarin Schiff bases, Journal of Coordination Chemistry. 2011;64(24):4264–4275.

11. Abel-Olaka LO, Kpee F, Festus C. Solvent extraction of 3d metallic elements using N_2O_2 Schiff Base-Chelators: Synthesis and Characterization, Nigerian Research Journal of Chemical Sciences. 2019;7(2):291-307.
Available:http://www.unn.edu.ng/nigerian-research-journal-of-chemical-sciences/ 196

12. Nnenna WO, Festus C, Muhammad AD. Synthesis, adsorption and inhibition behaviour of 2-[(thiophen-2-ylmethylidene)amino] pyridine-3-ol on mild steel corrosion in aggressive acidic media" Nigerian Research Journal of Chemical Sciences. 2020;8(2):291-307.
Available:http://www.unn.edu.ng/nigerian-research-journal-of-chemical-sciences/ 291

13. Festus C, Anthony CE, Osowole AA, Lukman OO, Damian CO, Oguejiofo TU. Synthesis, experimental and theoretical characterization and antimicrobial studies of some Fe(II), Co(II) and Ni(II) complexes of 2-(4,6-dihydroxypyrimidin-2-ylamino)naphthalene-1,4-dione" Research on Chemical Intermediates. 2018;44(10):5857-5877.
DOI: 10. 1007/s11164-018-3460-7

14. Osowole AA, Festus C. Synthesis, characterization, antibacterial and antioxidant activities of some heteroleptic Metal(II) complexes of 3-{[-(pyrimidin-2-yl)imino]methyl}napthalen-2-ol, Journal of Chemical, Biological and Physical Sciences. 2015;6(1):080-089.
Available:www.jcbsc.org

15. Festus C, Anthony CE, Osowole AA, Sunday ON, Collins UI, Damian CO, Oguejiofo TU. Synthesis, characterization, in-vitro antimicrobial properties, molecular docking and DFT studies of 3-{(E)-[(4,6-dimethylpyrimidin-2-yl)imino]methyl}naphthalen-2-ol and Heteroleptic Mn(II), Co(II), Ni(II) and Zn(II) complexes, Open Chem. 2018;16:184–200.
Available:https://doi.org/10.1515/chem-2018-0020

16. Festus C, Ibeji CU, Okpareke O. Novel 3d divalent metallic complexes of 3-[(2-hydroxy-5-methylphenylimino)-methyl]-napthalen-2-ol: Synthesis, spectral, characterization, antimicrobial and computational studies" Journal of Molecular Structure. 2020;1210:1-13.

17. Cotton FA, Wilkinson G. Advanced Inorganic Chemistry. Wiley Eastern Limited: New Delhi; 1978.

18. Lever ABP. Inorganic Electronic spectroscopy. 4th Ed. Elsevier publishing, Amsterdam: The Netherlands; 1980.

19. Figgis BN. Introduction to ligand field, Interscience. New York; 1969.

20. Salmon L, Molnar G, Cobo S, Oulié P, Etienne M, Mahfoud T, Demont P, Eguchi A, Watanabe H, Tanaka K, Bousseksou A. Reinvestigation of the spin crossover phenomenon in the ferrous complex $[Fe(HB(pz)_3)_2]$, New Journal of Chemistry. 2016;33(6):1283-1289.

21. Cotton FA, Wlkinson G, Murillo CA, Bochmann M. Advanced Inorganic Chemistry, 6^{th}.Ed. John wiley: New York; 1999.

22. Day (jr) MC, Selbin J. Theoretical Inorganic Chemistry, 2^{nd} Ed. Litton Educational Publishing; 1969.

23. Gaber M, Mabrouk HE, Al-Shihry S. Complexing behaviour of naphthylidenesulfa methazine Schiff base ligand towards some metal ions, Egyptian J. Chem. 2001;44:191-200.

24. Osowole AA, Oni AA, Onyegbula K, Hassan AT. Synthesis, spectral, magnetic and in-vitro anticancer properties of some metal(II) complexes of 3-[2,4-dihydro-1H-inden-4-ylimino) methyl]napthalene-2-ol. International Research Journal of Pure and Applied Chemistry. 2012;2(3):211–220.

25. Akrawi BA, Ali AM. The Electrical Conductivity of Some Transition Metal Complexes with 2,2'-Bipyridyl in Different Solvents at 298. 16K. Nat. J Chem. 2008;31:491-500.

26. Ajibade PA, Idemudia OG. Synthesis, characterization and antibacterial studies of Pd(II) and Pt(II) complexes of some

diaminopyrimidine derivatives. Bioinorg. Chem. Appl. 2013;2013:1–8.
Available:https://doi.org/10.1155/2013/549549

27. Festus C. Synthesis, Characterization and Antibacterial Studies of Heteroleptic Co(II), Ni(II), Cu(II) and Zn(II) Complexes of N-(2-hydroxybenzylidene)pyrazine-2-carboxamide. International Journal of Chemistry, Pharmacy & Technology. 2017;2(5):202-211.
Available:https://www.ics.ir/Files/Content/Media/15775-20170912110005
28. Lever ABP. Inorganic Electronic spectroscopy". Elsevier publishing, London: New York; 1986.
29. Osowole AA, Ott I. Synthesis, characterization, in-vitro anticancer and antimicrobial properties of some metal (II) complexes of 4-[(2,3-dihydro-1H-inden-4- ylimino) methyl] benzene-2,4-diol. International Research Journal of Pure and Applied Chemistry. 2012;2:156-169.
DOI: 10.9734/IRJPAC/2014/1541
30. Anitha C, Sumathi S, Tharmaraj P, Sheela CD. Synthesis, Characterization, and Biological Activity of Some Transition Metal Complexes Derived from Novel Hydrazone Azo Schiff Base Ligand International Journal of Inorganic Chemistry. 2011;2011.
DOI: 10.1155/2011/493942
31. Osowole AA, Festus C. Synthesis, characterization and antibacterial activities of some metal(II) complexes of 3-(-1-(2-pyrimidinylimino)methyl-2-napthol, Elixir Appl. Chem. 2013;59:15843-15847.
Available:www.elixirpublishers.com
32. Mahendra RK, Vivekanand B, Mruthyunjayaswamy B, Hire M. Synthesis, Characterization, Antimicrobial, dna cleavage, and antioxidant studies of some metal complexes derived from schiff base containing indole and quinoline moieties, Bioinorganic Chemistry and Applications. 2013;2013.
Available:http://dx.doi.org/10.1155/2013/315972
33. Kpee F, Ukachukwu CV, Festus C. Synthesis, Characterization and extractive potentials of aminopyrimidine schiff base ligands on divalent metal ions, Nigerian Research Journal of Chemical Sciences. 2018;4(2):193-203.
Available:http://www.unn.edu.ng/nigerian-research-journal-of-chemical-sciences/193
34. Esmadi FT, Khabour OF, Abbas K, Mohammad AE, Obeidat RT, Mfady D. Synthesis, characterization and biological activity of some unsymmetrical Schiff base transition metal complexes, Drug and Chemical Toxicology. 2015;39(1):41-47.
DOI: 10.3109/01480545.2015.1017882
35. Hadi AR, Mohammad RI, Moazam V, Askari B, Khorshidifard M, Habibi N, Bruno G. Synthesis, characterization, X-ray crystal structures and antibacterial activities of Schiff base ligands derived from allylamine and their vanadium(IV), cobalt(III), nickel(II), copper(II), zinc(II) and palladium(II) complexes, Journal of Molecular Structure. 2016;2016.
Available:http://dx.doi.org/10.1016/j.molstruc.2016.06.055
36. Cater AP, Clemons WM, Brodersen DE, Morgan-Warren RI, Wimberly BT, Ramakrishnan V. Functional insights from the structure of the 30S ribosomal subunit and its interactions with antibiotics. Nature. 2000;407(6802):340-348.
37. Thangadurai TD, Natarajan K. Mixed ligand complexes of ruthenium(II) containing α, β unsaturated-β-ketoamines and their antibacterial activity Trans Met Chem. 2001;26:500–504.
Available:https://doi.org/10.1023/A:1011099517420
38. Murukan B, Mohanan K. Synthesis, characterization and antibacterial properties of some trivalent metal complexes with [(2-hydroxy-1-naphthaldehyde)-3-isatin]-bishydrazone, Journal of Enzyme Inhibition and Medicinal Chemistry. 2007;22(1):65-70.
DOI: 10.1080/14756360601027373
39. Festus C, Okafor SN, Ekennia AC. Heteroleptic Metal Complexes of a Pyrimidinyl Based Schiff Base Ligand Incorporating 2,2′-Bipyridine Moiety: Synthesis, Characterization, and Biological Studies, Front. Chem. 2019; 7(862):1-12.
DOI: 10.3389/fchem.2019.00862